

SMOOTH PIECEWISE ALGEBRAIC APPROXIMATION AS APPLIED TO LARGE-SCALE 2D SCATTERED GEODETIC DATA FITTING

Azadeh Koohzare, Petr Vaníček, Marcelo Santos

Department of Geodesy and Geomatics Engineering, University of New Brunswick,
P.O. Box 4400, Fredericton, NB, Canada. E3B 5A3

ABSTRACT

We have developed an efficient method, Smooth Piecewise Algebraic Approximation (hereafter SPAA), to automatically compute a smooth approximation of large-scale functional scattered 2D observation points and tilt between them. The area of study is divided into patches and piecewise algebraic surfaces are fitted to the data. When the surfaces are approximated, a set of constraints is imposed in such a way that the resulting function is continuous only in the zero and first derivatives everywhere in the region, which results in a very short computation time. In other words, the surfaces are fitted simultaneously, using the constraints as set-conditions which the parameters of the surfaces must also satisfy. This method does not require a triangulation or quadrangulation of the data points and as such, it is very well suited for extremely large datasets.

This method has been successfully applied to the monthly mean sea level and re-levelling data in Canada to thereby compile a map of Vertical Crustal Movements (VCM) in the region. The VCM model obtained using this method accommodates different kinds of scattered geodetic data, while yielding the optimum approximation to them. Enforcing the continuity and smoothness throughout the surfaces, the VCM model of Canada highlights the long wavelength temporal variations of the crust in the region, mainly due to Post Glacial Rebound (PGR). As a result, using the method of SPAA, a more physically meaningful VCM is modelled.

KEYWORDS: Scattered data fitting. Piecewise functions. Functional constraint. Geodetic data fitting.

INTRODUCTION

In order to predict the spatial vertical velocities, or uplift rates, a vertical velocity surface should be fitted to the scattered data of sea level linear trends and rate of levelling height differences (tilt). The problem of functional scattered geodetic data fitting can be described as follow: Given two sets of pairing points and individual points:

$$\begin{aligned} \{(x_i, y_i), (x_j, y_j)\} &\in \Omega, i = 1, \dots, N, j = 1, \dots, N \\ (x_t, y_t) &\in \Omega, t = 1, \dots, p, \end{aligned} \quad (1)$$

Where Ω is a bounded domain in the plane. Their corresponding values $\Delta V_{ij} = V_j - V_i$, $i, j = 1, \dots, N$ and V_t , $t = 1, \dots, p$, are also given as the relative and absolute vertical velocities, respectively. We want to find a method to construct a surface $S : \Omega \mapsto R$ that meets as many as possible of the following goals:

- Approximation: S should approximate different types of data while offering least square approximation.

$$\begin{aligned} \{S(x_j, y_j) - S(x_i, y_i)\} &\approx \Delta V_{ij} (i, j = 1, \dots, N). \\ S(x_t, y_t) &\approx V_t (t = 1, \dots, p). \end{aligned} \quad (2)$$

- Quality: S should be of high visual quality (i.e., S should be continuous and smooth) and have convenient properties for further processing.

- **Independency:** the method should be independent of the choice of *nodal points*.
- **Usability:** large number of geodetic data, where N is typically of the order of 10^5 , should be manageable.
- **Stability:** the computation of S should be numerically stable, i.e., the method should work for any distributions of scattered points.
- **Adaptiveness:** the local variation and distribution of the data should be taken into account.
- **Simplicity:** the method should be easy to implement.

Although many approaches have been developed mainly in mathematics and computer sciences, (see for instance the survey and overview in [8], [17], [21]), the literature shows that it is a difficult task to meet all of the above goals by using one single method. Of utmost limitation of all the methods is that they can not be used for different types of data, point values and relative values (tilt) between points. Other limitations are severe restrictions on the number of data, restriction on the domain and distribution of the data and a limitation to handle large linear equation systems [11]. In order to review the related works, we have divided the methods of data fitting into two groups: 1- fitting a unified surface to the data, 2- fitting piecewise surfaces. In the following, some of these methods and the advantages and limitations of each technique in the context of Vertical Crustal Movements (VCM) are discussed.

UNIFIED SURFACE FITTING TO THE DATA

The main idea is to provide an approximation surface, $S(x, y)$, to the data. Generally, the surface can be expressed as:

$$S(x, y) = \sum_{i=1}^l c_i \psi_i(x, y). \quad (3)$$

where ψ_i are some arbitrarily chosen, linearly independent functions (basis functions) of the position and c_i are the best fitting coefficients to the observations [33].

Different models can be produced by choosing different suitable basis functions. All of them have their own advantages and disadvantages and are appropriate to different deformation behaviours. Practically, the two dimensional algebraic functions would be used in most cases. The basic equation then becomes

$$S(x, y) = \sum_{i,j=0}^n c_{ij} x^i y^j, \quad (4)$$

where n is the degree of the polynomial, and c_{ij} are the sought coefficients [35]. Here, the algebraic functions are the simplest functions to deal with numerically and are adequate when the solution is confined to the regions where sufficient data exists; the poor behaviour appears only when the solution is used in an extrapolation mode. These models are more applicable in the compilation of a map of VCM as they can use both point and tilt data. In other words, different types of the data are used in one model. To get the details needed for the map to be meaningful, the order of the velocity surface would have to be too high to be numerically manageable. This would cause wild oscillations (artifacts) where there are no data.

The radial basis methods are another active area of research for scattered point fitting [6]. Generally, by a radial function, we mean a function:

$$g : R^d \rightarrow R : (x_1, x_2, \dots, x_d) \mapsto \phi(\|x_1, x_2, \dots, x_d\|_2), \quad (5)$$

for some function $\phi : R \rightarrow R$. Here d represents the dimension of the problem, i.e., $d=2$ in our case. In other words, the function value of g in a point $\bar{x} = (x_1, x_2, \dots, x_d)$ only depends on the L2-norm of \bar{x} . An example of such radial methods is the Multi Quadric method (MQ) [12]. This method considers the vertical crustal deformations as one kind of continuous changes which can be approached precisely by the superposition of Multi Quadric functions:

$$S(x, y; t - t^0) = \sum_{i=1}^k c_i K(x, y, x_i, y_i)(t - t^0). \quad (6)$$

where t is the present epoch of time; t^0 is the pre-specified initial epoch of time, K is the kernel function, i is its running number and k is the total number of kernel functions; c_i is the unknown coefficients. The general form of K is:

$$K(x, y, x_i, y_i) = [(x - x_i)^2 + (y - y_i)^2 + \delta^2]^b. \quad (7)$$

where (x_i, y_i) is the nodal point, δ is the smoothing factor, b is selected to determine the form of the function; usually, it is chosen to be equal to 1, $\frac{1}{2}$ or $-\frac{1}{2}$, etc. [19]

Special attention should be paid to the location of nodal points, which indeed controls the pattern of the surface. This method strongly depends on the choice of (x_i, y_i) , and while dealing with tilt data, deciding about where to choose the nodal points is nontrivial. Figures 1a, b show how effectively the nodal point control the pattern of the surface. In this figure, two different sets of nodal points were considered for the computation, each consists of 18 points.

Another problem is that these methods usually require solving large, ill-conditioned linear system. Therefore, sophisticated iterative techniques are needed for the computation of the radial function interpolants [11].

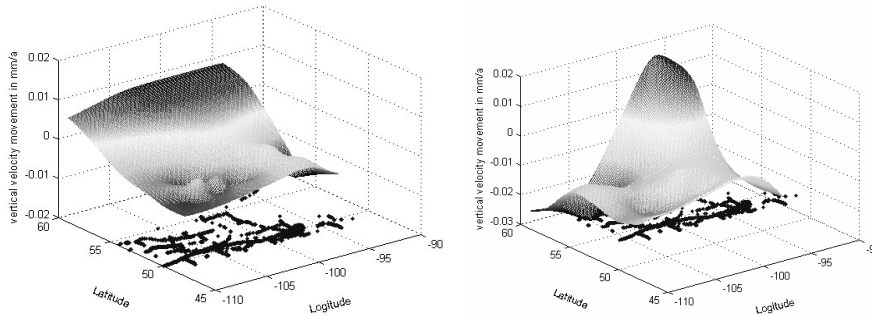


Fig. 1. The vertical velocity surfaces obtained using the MQ analysis, using two different sets of nodal points. The blue dots show the location of data points.

PIECEWISE FITTING METHODS

A practical way to avoid the problem of wild oscillations due to using a unified surface is to divide the area of study into pieces, and seek the velocity surface piecewise. One of the most common methods in this area is the use of Free-form Blending [24]. In this approach, the fitting is performed locally and the results are

merged to form a global approximation (See for example [30], [14]). These methods are fast and easy when there are dense data, but in the sense of sparse data, would not be applicable [14]. On the other hand, the function value in each vertex is to be known, while in geodetic datasets, the point values are available only in some of the elements.

Another common approach is the use of splines. There are several types of splines that can be used. The simplest approach in data fitting using splines is to apply tensor product splines [5],[7],[10],[9]. In general, the tensor product methods are straightforward to apply only for the data given on a grid [11]. Parametric bicubic splines are adoptively subdivided to approximate 3D points with a regular quadmesh structure [11], and multilevel B-splines are used to approximate functional scattered data points [18]. Other spline methods are based on simplex splines or splines of finite-element type [36]. The simplest example of finite element splines are continuous piecewise linear functions with respect to a suitable triangulation of the planar domain. It is well-known that these methods which are based on piecewise linear functions can not exceed the approximation order 2. To achieve a higher smoothness and approximation order, polynomial patches of the greater degree have to be considered.

In particular, there are scattered data methods based on classical smooth finite elements such as the Bell quintic element, Frajies de Veubecke-Sander and Clough-Tocher cubic elements, and Powell-Sabin quadratic element (see the above-mentioned surveys and more recent papers [3],[5],[25]. The above-mentioned methods based on finite elements require accurate estimates of the derivatives at the data points, which is a nontrivial task by itself assuming the data points are irregularly distributed. To overcome these difficulties, a global least squares approximation and other global methods are considered [5],[22],[36].

The basic idea of the method used in this research is related to the approximation scheme of [33]. An essential difference is, however, that piecewise polynomials are used. This method is different from the standard spline, as the data points are neither triangulated (or quadrangulated), nor any interpolation scheme as for instance in [3] and [25] are used. In particular, there is no need of any pre-estimates of functional values at points different from the given data points. Instead, local least squares approximations are computed, directly in the polynomial form and then the remaining degrees of freedom are settled by continuity conditions, which results in very short computation times. Since this method does not even require a triangulation of the data points, it is very well suited for extremely large datasets. Theoretical aspects of the method are discussed in the following.

SMOOTH PIECEWISE ALGEBRAIC APPROXIMATION

The procedure of fitting a surface to the geodetic data involves the use of both the point rates and the gradients simultaneously, together with their proper weights. The point rates are determined from some of the tide gauge data which were selected to be used in the point velocity mode, and the gradients come from re-levelled segments and tide gauge pairs.

In order to fit a surface to the geodetic data, it is advantageous first to transform the geodetic coordinates of φ and λ to rectangular coordinates x and y related to an arbitrary origin located to the centre of the region as

$$\begin{aligned} x &= R(\lambda - \lambda_0) \cos \varphi \\ y &= R(\varphi - \varphi_0) \end{aligned} \quad (8)$$

Here, x and y are the easting and northing in a local Cartesian system, R is the Gauss radius of curvature, φ_0 and λ_0 are the geodetic coordinates of the origin of the grid. In general, we divide the area of study into p patches. A given polynomial in the m^{th} ($m=1, 2, \dots, p$) patch looks as follows:

$$V_m(x, y) = \sum_{i=0}^{n_x} \sum_{j=0}^{n_y} c_{ij,m} (x - x_{0m})^i (y - y_{0m})^j \quad (9)$$

where V_m is the algebraic least squares velocity surface for patch m , fitted to the desired data (x, y) . The pair (x_{0m}, y_{0m}) represents the position of the origin in patch m and $c_{ij,m}$ are the unknown coefficients in patch m .

If m and m' represents the two adjacent patches having common border mm' (Figure 2), then in order to piece the polynomials together, the following conditions must be satisfied:

$$V_m(x_{mm',k}, y_{mm',k}) = V_{m'}(x_{mm',k}, y_{mm',k}) \quad \forall k = 1, 2, \dots, q \quad (10a)$$

$$\left. \frac{\partial V_m(x, y)}{\partial x} \right|_{\substack{x=x_{mm',k} \\ y=y_{mm',k}}} = \left. \frac{\partial V_{m'}(x, y)}{\partial x} \right|_{\substack{x=x_{mm',k} \\ y=y_{mm',k}}} \quad \forall k = 1, 2, \dots, q \quad (10b)$$

$$\left. \frac{\partial V_m(x, y)}{\partial y} \right|_{\substack{x=x_{mm',k} \\ y=y_{mm',k}}} = \left. \frac{\partial V_{m'}(x, y)}{\partial y} \right|_{\substack{x=x_{mm',k} \\ y=y_{mm',k}}} \quad \forall k = 1, 2, \dots, q \quad (10c)$$

$(x_{mm',k}, y_{mm',k})$ is the position of k^{th} nodal point in the border mm' joining patches m and m' . Here, q represents the maximum number of the nodal points in the common border between patch m and patch m' .

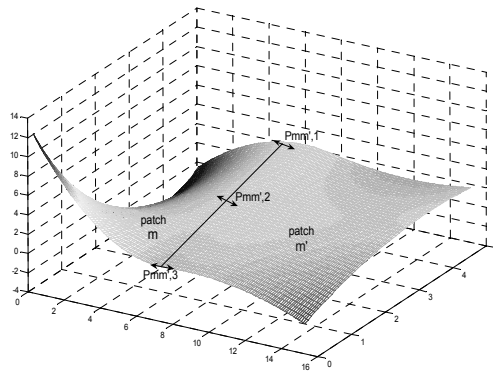


Fig. 2. Two adjacent patches m and m' and the nodal points in the common border between two patches $(P_{mm',1}, P_{mm',2}, \dots, P_{mm',k=q})$

The conditions (10a) make sure that the piecewise polynomial fits to the nodal points $(P_{mm',1}, P_{mm',2}, \dots, P_{mm',k=q})$ located in the predefined border mm' between two patches m and m' . These conditions imply that the function is continuous everywhere in the region. Conditions (10.b) and (10.c) ensure that the polynomials are continuous in slope along x and y directions, respectively. The main mathematical model is Eq. (9) while all the conditions of Eq. (10) show the existence of constraints on the main model [16].

One can rewrite Eq. (9) in a more suitable form for the velocity differences between two adjacent bench marks A and B (tilt).

$$\Delta V_m(x_A, y_A, x_B, y_B) = \sum_{i=0}^{n_x} \sum_{j=0}^{n_y} c_{ij,m} [(x_B - x_{0m})^i (y_B - y_{0m})^j - (x_A - x_{0m})^i (y_A - y_{0m})^j]. \quad (11)$$

The ‘observations’ on the left hand side of the equation are used to compute the coefficients by means of the least-squares method. To find the least square solutions, Eqs. (10) and (11) can be simplified in a general form:

$$f(\mathbf{c}, \mathbf{I}) = 0, \quad (12a)$$

$$f_c(\mathbf{c}) = 0. \quad (12b)$$

Here, \mathbf{I} is the vector of observations which includes $V_m(x_t, y_t)$ from the tide gauge observations and $\Delta V_m(x_A, y_A, x_B, y_B)$ from the re-levelling data and paired tide gauges. \mathbf{c} is the vector of unknown coefficients. It is assumed to be possible to solve for \mathbf{c} , using only the main model of Eq. (12a). The auxiliary model f_c consists of the constraint functions that are enforced. The above models are then linearised to yield:

$$\begin{aligned} \mathbf{A}\delta + \mathbf{B}\mathbf{r} + \mathbf{w} &= 0, \\ \mathbf{D}\delta + \mathbf{w}_c &= 0. \end{aligned} \quad (13)$$

with $\text{rank}(\mathbf{A})=u$ $\text{rank}(\mathbf{B})=c$ and $\text{rank}(\mathbf{D})=d$.

In Eqs. (10), \mathbf{r} is the vector of the expected residuals. The matrices \mathbf{A} and \mathbf{D} are the Jacobian matrices of transformation from the parameter space to the two model spaces, valid for a small neighborhood of $\mathbf{c}^{(0)}$. The matrix \mathbf{B} is the Jacobian matrix of the transformation from the observation space to the main model space. It is observed that Eqs. (13) are merely the differential form of the original non-linear mathematical model Eqs. (12a) and (12b) and describe the relations of the quantities in the neighborhoods of $\mathbf{c}^{(0)}$, the point of expansion in the parameter space, and $\mathbf{w}^{(0)}$, the misclosure vector, where,

$$\begin{aligned} \delta &= \mathbf{c} - \mathbf{c}^{(0)}, \\ \mathbf{w}^{(0)} &= f(\mathbf{I}^{(0)}, \mathbf{c}^{(0)}). \end{aligned} \quad (14)$$

In the presence of constraints, it is, in general, possible that $u > c$ leading to rank of \mathbf{A} being c . In such a situation, part of the development to follow (solution by partitioning) would not work. Therefore, we assume that $u < c$. The tasks of constrained fitting can now be formulated. The standard method for solving a minimisation problem subject to a set of constraints is the use of Lagrangian multipliers. The constraints $f_c(\mathbf{c}) = 0$ are viewed as a hypersurface S upon which we wish to minimise $f(\mathbf{c}, \mathbf{I}) = 0$. The variation function for finding the least-squares solution is written as,

$$\phi = \mathbf{r}^T \mathbf{C}_r^{-1} \mathbf{r} + 2\mathbf{k}^T (\mathbf{A}\delta + \mathbf{B}\mathbf{r} + \mathbf{w}) + 2\mathbf{k}_c^T (\mathbf{D}\delta + \mathbf{w}_c), \quad (15)$$

where $\mathbf{C}_r = \mathbf{C}_l$ is the covariance matrix of the observations. Here, there are two sets of Lagrange correlates: \mathbf{k} , \mathbf{k}_c , reflecting the fact that two models are present. The minimum with respect to \mathbf{r} is found by the Lagrange approach [23],[34] as

$$\hat{\boldsymbol{\delta}} = \boldsymbol{\delta}^{(0)} - \mathbf{N}^{-1} \mathbf{D}^T (\mathbf{D} \mathbf{N}^{-1} \mathbf{D}^T)^{-1} (\mathbf{w}_c + \mathbf{D} \boldsymbol{\delta}^{(0)}), \quad (15)$$

where

$$\mathbf{N} = (\mathbf{A}^T (\mathbf{B} \mathbf{C}_r \mathbf{B}^T)^{-1} \mathbf{A})^{-1} \quad (16)$$

$$\mathbf{u} = \mathbf{A}^T (\mathbf{B} \mathbf{C}_r \mathbf{B}^T)^{-1} \mathbf{w} \quad (17)$$

$$\boldsymbol{\delta}^{(0)} = -\mathbf{N}^{-1} \mathbf{u} \quad (18)$$

Eq. (19) represents the solution from the main model f alone. The corrective term $\hat{\boldsymbol{\delta}} - \boldsymbol{\delta}^{(0)}$ in Eq. (16) arises from the enforcement of the constraints.

SEQUENTIAL CONSTRAINTS SATISFACTION

The Lagrangian-multiplier method works adequately when the constraints are independent, but is less useful when they are not [1]. In this work, a sequential approach to select the optimum number of independent constraints is used. We assume that the constraints have been sorted into an order of priority: $f_c(\mathbf{c}) = (\mathbf{c}_1, \mathbf{c}_2, \dots, \mathbf{c}_k)$, where \mathbf{c}_1 is a vector of highest priority constraints, and \mathbf{c}_k the lowest. We wish to find for $f(\mathbf{c}, \mathbf{l}) = 0$, by sequentially attempting to satisfy the constraints in their priority order.

The two problems: $f(\mathbf{c}, \mathbf{l}) = 0$ and $f_c(\mathbf{c}) = 0$ are solved simultaneously using the Lagrangian-multiplier method (see previous section) with more sets of constraints in different steps. Depending on the desired degree of freedom for the resulting velocity surface, while still securing the regular solutions, the computations end at that step.

TESTING THE ERRORS

The next task is to obtain the covariance matrix $\hat{\mathbf{C}}_{\hat{\boldsymbol{\delta}}}$ of the parameters. This is given by [23],[34] as:

$$\hat{\mathbf{C}}_{\hat{\boldsymbol{\delta}}} = \mathbf{N}^{-1} - \mathbf{N}^{-1} \mathbf{D}^T (\mathbf{D} \mathbf{N}^{-1} \mathbf{D}^T)^{-1} \mathbf{D} \mathbf{N}^{-1}. \quad (19)$$

The appropriate degree of the resulting surface is determined by testing the estimated accuracy, or the ‘a posteriori variance factor’. The latter is computed from

$$\hat{\sigma}_0^2 = \frac{\hat{\mathbf{r}}^T \mathbf{C}_l^{-1} \hat{\mathbf{r}}}{\nu}. \quad (20)$$

where $\hat{\mathbf{r}}$ is the vector of the least square estimation of the residuals and ν denotes the number of degrees of freedom

FILTERING THE SOLUTION

Some of the computed coefficients may not be statistically significant on a certain level of probability and they should be filtered out in the first stage. In order to discard all the coefficients that are not significantly different from zero, one way is to orthogonalise the basis. Then each of the coefficients can be tested for statistical significance against its own variance. A certain level of significance, in terms of a multiple of the standard deviation can be assumed, and all the coefficients, insignificant on this level, can be discarded. Here, the Gram-Schmidt orthogonalisation is applied to the polynomial basis $(\psi_i(\varphi, \lambda))$, the significance tests for the coefficients is performed, and the solution is de-orthogonalised into the natural solution space [32]. The basis functions in Eq. (3), can be written as

$$\Psi \equiv \{\psi_1, \psi_2, \dots, \psi_l\}. \quad (21)$$

The above bases are then orthogonalised to obtain

$$\Psi^* \equiv \{\psi_1^*, \psi_2^*, \dots, \psi_l^*\}. \quad (22)$$

The coefficients for each individual patch are then evaluated in the orthogonal space as

$$\delta^{(1)*} = \left[\langle \psi_i^*, \mathbf{w} \rangle / \|\psi_i^*\|^2; i=1, \dots, l \right]. \quad (23)$$

These coefficients should be confirmed as significant. To test their significance, one can start from the following null hypothesis:

$$H_0 : E(\delta_i^{*(1)}) = 0; i=1, \dots, l. \quad (24)$$

where $\delta_i^{*(1)}$ is the i^{th} coefficient for each patch, computed in the orthogonal space. It is therefore possible to define a statistic that, if H_0 is true, follows a t (Student) distribution [2],[34]:

$$-t_{\beta, \nu} < \frac{\delta_i^{*(1)}}{\sigma_{\delta_i^{*(1)}}} < t_{\beta, \nu}, \quad (25)$$

where $\sigma_{\delta_i^{*(1)}}$ is the standard deviation of $\delta_i^{*(1)}$ and ν is the degree of freedom, i.e., the number of redundant observations. The hypothesis H_0 is accepted or rejected depending on whether the absolute value t_0 is smaller or greater than a boundary value t_{β} at a chosen confidence level [2],[34],[19]. When H_0 is found valid, $\delta^{*(1)}$ should be rejected. Otherwise, $\delta^{*(1)}$ should remain in the model. After discarding the non-significant coefficients from Eq. (21), we de-orthogonalise Eq. (21) into the natural space by

$$\delta^{(1)} = \mathbf{T}^t \delta^{*(1)}. \quad (26)$$

Here \mathbf{T} is the transformation matrix from orthogonalised space to non-orthogonalised space.

In order to fit a simultaneous surface to 2D measured data and the tilts between them in an “automatic” process, it was decided to divide the area of study into patches with regular shapes. In this study, some square and rectangular patches with different sizes were selected in which the border between two adjacent patches is always a straight line parallel to one of the coordinate axis. This way, the number of constraints for the continuity and smoothness would be reduced and consequently a higher degree of freedom would be achieved. Another advantage is that when dealing with a high number of data, this approach is more adoptable.

Therefore, the region of study, Canada, was divided into patches of different sizes depending on the number and the distribution of the data. The size of the patches was initially selected to be 2×2 degree and if there were not enough data in a particular patch, or the data were not well distributed, the adjacent patches were combined to create a bigger patch. This was done automatically in the Program SPAA-VCM by checking the number of data. Figure 3 shows the selection of the patches and the combinations of some of them.

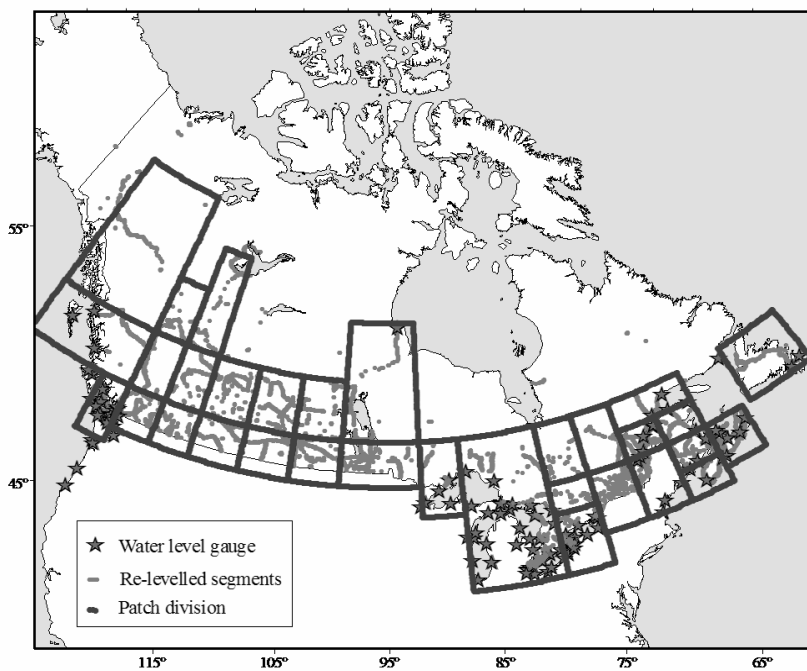


Fig. 3. The selection of the patches and their combinations.

The next step was to seek the vertical movement by different polynomial surfaces in each patch. The polynomials were joined together at the nodal points on the boundaries of the patches in such a way that a desired degree of smoothness (differentiability) of the resulting function was guaranteed. In this work, the continuity and smoothness conditions (Eqs. 10a, 10b, 10c) were satisfied.

Several tests were made to determine the appropriate degree of the velocity surface to be computed for each patch. As an example, Table 1 shows the *a posteriori* variance factors for the degrees 2, 3 and 4 for a sample area in Eastern Canada (please see [16] for more details). All degrees of the polynomials yielded *a posteriori* variance factors between 8.1-8.5. The value $n=3$ was finally selected as the highest degree compatible with the data distribution in that area [16].

Table 1. *A posteriori* variance factors of polynomial surfaces of degree 2, 3 and 4 for a sample patch in Eastern Canada [16]

Degree of polynomials	Degree 2	Degree 3	Degree 4
a posterior variance factor	8.4	8.1	8.3

NUMERICAL INSTABILITIES

One of the basic concepts that should be discussed before explaining the numerical problems is the notion of the sensitivity to the data distribution. We wish to solve a numerical problem that arises from a practical setting, say solve $\mathbf{Ac} = \mathbf{l}$, where \mathbf{A} is a square matrix and \mathbf{l} is the observed vector, and \mathbf{c} is the vector of unknown coefficients. It is well-known that there is a unique solution if and only if matrix \mathbf{A} is regular. Mathematically, there is nothing more to say. However, practically it is very important to know how sensitive the solution \mathbf{c} is to perturbations in the data distribution which are presented in matrix \mathbf{A} . If the mathematical solution is very sensitive to changes in the data distribution (i.e., the problem may be poorly conditioned) then it is not possible to guarantee that the computed solution is correct. Overdetermined systems of linear equations behave the same. If the problem is poorly conditioned, we may not find the unknown coefficients such that \mathbf{Ac} is 'close' to \mathbf{l} (in the least squares sense).

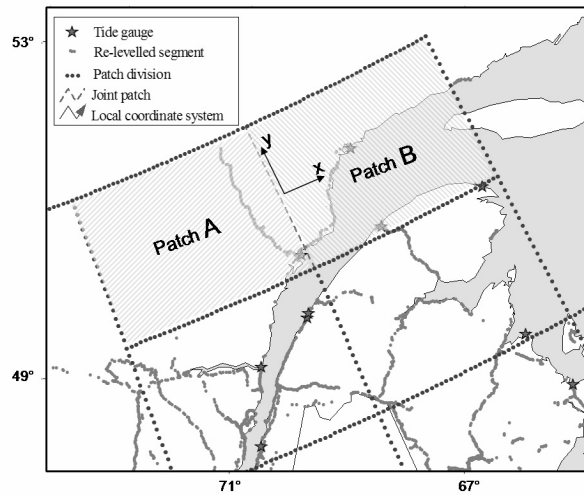


Fig. 4. Data distribution in two adjacent patches (A, B) which are ultimately joined together to avoid ill-conditioned systems.

One frequent problem in VCM modelling using SPAA is that the system of normal equations might be ill-conditioned, which means that the solution is hypersensitive to

changes in the position of the data. This is the case especially for the initial solutions in patches with a poor distribution of data. For example in two adjacent patches, one (A) 49°-51° North and 64°-68° West, and the other (B) 49°-51° North and 68°-72° West, there are 106 and 101 observation equations, respectively (Fig. 4). Theoretically, the system could be solved, with a reasonable number of degrees of freedom. However, due to the poor distribution of the data (all along one line), the matrices of observations are ill-conditioned.

One remedy is to combine the patch with a poor distribution of data with adjacent patch or patches, to create a patch with a more reasonable distribution of the data. In Figure 4, two adjacent patches (A, B) are joined to make patch A+B. In order to secure a numerical stability of the solution, the origin of the coordinate system should be chosen carefully.

To see the effect of different origins of coordinate systems on the standard deviation of the absolute term of the VCM in patch A+B, a cubic polynomial surface was fitted to the data in the patch (Figure 4). The origin of the coordinate system for the computation was assigned (1) outside the patch, (2) in the centre of the patch, (3) in the centre of mass of the data in the patch. Three different solutions were obtained and the covariance matrices for the computed coefficients were calculated. Table 2 shows the standard deviations of the absolute term of the VCM computed in patch A+B in three different coordinate systems.

Table 2. *Standard deviation of the absolute term of the VCM computed in patch A+B in three different coordinate systems.*

The origin of the coordinate system	Standard deviation of the absolute term of the VCM (mm/year)
1-Outside the Patch $\varphi_s=46^{\circ}00'00''$, $\lambda_s=79^{\circ}00'00''$	553.0
2-Centre of the Patch $\varphi_s=50^{\circ}00'00''$, $\lambda_s=68^{\circ}00'00''$	0.52
3-Centre of the mass $\varphi_s=49^{\circ}43'48''$, $\lambda_s=67^{\circ}55'12''$	0.39

The standard deviation of the absolute term for the VCM in this patch strongly depends on the location of the origin of the coordinate system. This is mainly due to the poor distribution of the data which made the design matrix poorly conditioned. For the modeling of the VCM, it was decided to choose the origin of the coordinate system of each patch in the centre of that patch itself or, where necessary, in the centre of mass of the data of the patch.

RESULTS

The final map is the patchwork of 33 patches, and the cubic polynomials in most of the patches. The map of the VCM in Canada compiled using SPAA, which is confined to the distribution of data in the area, is illustrated in Figure 5. The map of the standard deviations of the computed VCM is shown in Figure 6.

The Post Glacial Rebound (PGR) hinge line, the zero line between rising and sinking land due to PGR, appears from the Gulf of St. Lawrence in the map of VCM (Figure 5). It follows the Atlantic coast line to the south of Canada. This gives some information about the deglaciation history of the ice model. The PGR hinge line then crosses the Great Lakes and continues westwards along the southern border between Canada and the U.S. and creates a dome shaped uplift in northern British Columbia (Figure 5). This map is in good agreement with the map of gravity changes in Canada [26], the Glacial Isostatic Adjustment (GIA) models [31],[27],[28] and the rate of

geodetic height changes of [29]. A comprehensive comparison between this map and the geophysical models, and the geodynamical interpretation of the map are presented in [15].

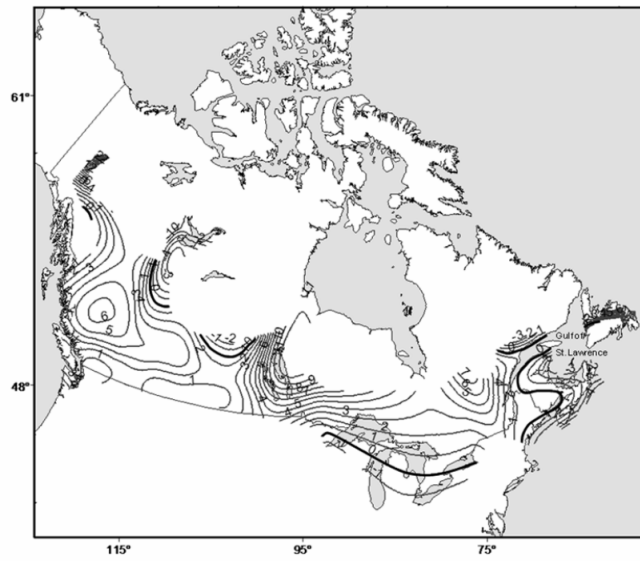


Fig. 5. Contour map of vertical crustal movements in Canada using Smooth Piecewise Algebraic Approximation. The Contours are in millimetre per year. The zero line is shown by thicker lines.

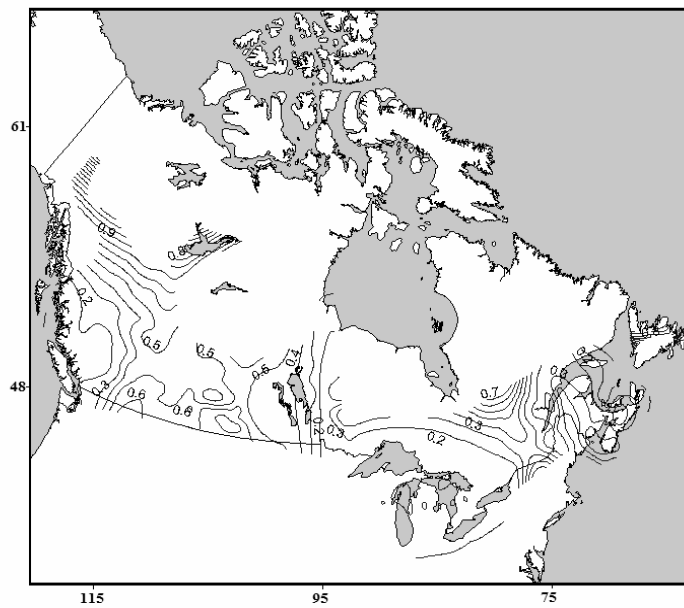


Fig. 6. Pattern of the standard deviation of the predicted Vertical Crustal Movements in Canada. Contours are in millimetre per year [15]

CONCLUSIONS AND RECOMMENDATION

The method of Smooth Piecewise Algebraic Approximation (SPAA) avoids many of the limitations associated with traditional approaches of data fitting such as the requirement that the data be of point values, as it is seen in the MQ method [12] and in B-splines [9],[10]; or they should be in grids or at least well distributed [36]. SPAA is not restricted to the low degree polynomials for all the patches by which a uniformly smooth surface throughout the region is maintained, as seen in [35]; instead the smoothness (differentiability) of the resulting function is guaranteed by imposing the constraints and the degree of smoothness can be simply controlled by the number and degree of differentiability constraints in the model. The Vertical Crustal Model (VCM) model developed in this research gives some details of the movements. Enforcing the continuity and smoothness in the first derivatives throughout the surface, the VCM model can highlight the long wavelength spatial variations of the crust in Canada, mainly due to Post Glacial Rebound (PGR). Moreover, our VCM model is independent to the choice of nodes. Even by having scattered data, and the ill-conditioned equation system in some patches, a stable solution can be manageable to be obtained by changing the coordinate system.

The use of SPAA was shown to be useful in compiling a map of VCM in Canada, where different types of data were utilised. Since surface modelling is needed in many applications in Geosciences, Surveying and other disciplines, and since geodetic data are usually distributed non-uniformly, it is strongly recommended that SPAA is used when dealing with scattered data of any types.

ACKNOWLEDGEMENT

We acknowledge financial support provided by GEOIDE (GEOmatics for Informed DEcisions) Network of Centers of Excellence of Canada and CIDA (Canadian International Development Agency).

References

1. Benko, P., Kos, G., Varady, T., Andor, L. and Martin, R., 2002. Constrained fitting in reverse engineering. *Computer Aided Geometric Design*, 19: 173- 205.
2. Crow, E. L., Davis, F. A., and Maxfield. M. W., 1960. *Statistics manual*. Dover, Mineola, NY.
3. Dahmen, W. A., Gmelig Meyling, R. H. J. and Ursem, J. H. M., 1990. Scattered Data Interpolation by Bivariate C^1 -piecewise Quadratic Functions. *Approximation Theory and its Applications*, 6: 6–29.
4. Dierckx, P. 1993. *Curve and Surface Fitting with Splines*. Oxford University Press.
5. Dierckx, P., S. Van Leemput, and T. Vermeire, 1992. Algorithms for Surface Fitting using Powell-Sabin Splines. *IMA Journal of Numerical Analysis*, 12 (2): 271–299.
6. Dyne, D. D. Levin, and Rippa, S., 1986. Numerical procedures for surface fitting of scattered data by radial functions. *SIAM Journal of Scientific and Statistical Computing*, 7(2): 639-659.
7. Forsey, D. R. and Bartels, R. H., 1995. Surface Fitting with Hierarchical Splines. *ACM Transactions on Graphics*, 14(2): 134–161.
8. Franke, R., 1982. Scattered data interpolation: test of some methods. *Mathematics of Computation*, 38(157), 181-200, January 1982.
9. Gregorski, B. F., Hamann, B., and Joy, K. I., 2000. Reconstruction of B-spline Surfaces from Scattered Data Points. *Proc. Computer Graphics International 2000*: 163–170.
10. Greiner, G. and Hormann. K., 1997. Interpolating and Approximating Scattered 3D

- Data with Hierarchical Tensor Product Splines. In A. Le Méhauté, C. Rabut, and L. L. Schumaker (eds.), *Surface Fitting and Multiresolution Methods*, Vanderbilt University Press, Nashville, 163–172.
11. Haber, J., Zeilfelder, F., Davydov, O. and Seidel, H. P., 2001. Smooth approximation and rendering of large scattered data sets. *Proceedings of the conference on Visualization '01* San Diego, California, 2001, 341 – 348. ISBN ~ ISSN: 1070-2385.
 12. Hardy, R. L., 1978. *The application of multiquadric equations and point mass anomaly models to crustal movements studies*. NOAA technical report NOS 76, NGS 11, Rockville, MD.
 13. Holdahl, R. S. and Hardy, R. L., 1978. Solvability and multiquadric analysis as applied to investigations of vertical crustal movements. *Tectonophysics*, 52 (1979): 139-155.
 14. Kobbelt, L. P., Bareuther, T. and Seidel, H. P., 2000. Multiresolution shape deformations for meshes with dynamics vertex connectivity. *Computer Graphics Forum*, 19(3): 249-259.
 15. Koohzare, A., Vaníček, P. and Santos, M., 2008. Pattern of recent vertical crustal movements in Canada, *Journal of Geodynamics*, 45 (2): 133-145.
 16. Koohzare, A., Vaníček, P. and Santos, M., 2006. The use of smooth piecewise algebraic approximation in the determination of vertical crustal movements in Eastern Canada. *Proc., Joint assembly of the IAG, IAPSO and IABO*, Cairns, Australia, Springer Verlag Press., 2005, 130.
 17. Lancaster, P. and Salkauskas, K., 1986. *Curve and Surface Fitting*. Academic Press.
 - 17A. Lang, S., 1987, *Linear Algebra, 3th ed.*, Springer Verlag NY Inc.
 18. Lee, S., Wolberg, G. and Shin, S. Y., 1997. Scattered Data Interpolation with Multilevel B-Splines. *IEEE Transactions on Visualization and Computer Graphics*, 3(3): 228–244.
 19. Liu, Q. W. and Chen, Y. Q., 1998. Combing the geodetic models of vertical crustal deformation. *Journal of Geodesy*, 72: 673-683.
 20. Liu, Q. W. and Parm, T., 1996. On the vertical deformation models. *Proc 8th FIG International Symposium on deformation measurements*, Hong Kong, 25-28 June.
 21. Lodha, S. K. and Franke, R., 1999. Scattered Data Techniques for Surfaces. In H. Hagen, G. Nielson, and F. Post, *Proc. Dagstuhl Conf. Scientific Visualization*, IEEE Computer Society Press: 182-222.
 22. Meyling, R. H. J. G and Pfluger, P. R., 1990. Smooth Interpolation to scattered data by bivariate piecewise polynomials of odd degree. *Computer Aided Geometric Design*, 7(5): 439-458.
 23. Mikhail, E. M., 1976. *Observations and least squares*, IEP, New York.
 24. Moore, D. and Warren, J., 1991. Approximation of dense scattered data using algebraic surfaces. *Proc. of the 24th Hawaii Intl. Conference on System Sciences*, 681-690, Kauai, Hawaii.
 25. Morandi, C. M., De Marchi, S. and Fasoli, D., 1999. A Package for Representing C^1 Interpolating Surfaces: Application to the Lagoon of Venice's Bed. *Numerical Algorithms*, 20(2, 3): 197–215.
 26. Pagiatakis, S. D., 2003. Historical relative gravity observations and the time rate of change of gravity due to postglacial rebound and other tectonic movements in Canada. *J. Geophys. Res.*, 108 (B9), 2406, doi: 10.1029/2001JB001676.
 27. Peltier, W. R., 1994. Ice Age Paleotopography. *Science*, 265: 195-201.
 28. Peltier, W.R., 2004. Global glacial isostasy and the surface of the ice-age earth: The ICE-5G (VM2) model and GRACE. *Annual Review of Earth and Planetary Sciences*, 32: 111-149. doi:10.1146/annurev.earth.32.082503.144359.
 29. Sella, G. F., Dixon, T. H. and Mao, A., 2002. REVEL: A model for recent plate velocities from space geodesy. *J. Geophys. Res.*, 107(B4), 2081, doi: 10.1029/2000JB000033.
 30. Turk, G., 1992. Re-tiling polygonal surfaces. In Edwin E. Catmull, editor, *Computer Graphics (SIGGRAPH '92 Proceedings)*, July 1992, 26: 55- 64.

31. Tushingham, A. M. and Peltier, W. R. (1991). Ice-3G: A new global model of late Pleistocene deglaciation based upon geophysical predications of postglacial relative sea level change. *J. Geophys. Res.*, 96: 4497-4523.
32. Vaniček, P., 1976. Pattern of recent vertical crustal movements in Maritime Canada. *Canadian Journal of Earth Sciences*, 13: 661-667.
33. Vaniček, P. and Christodulids, D., 1974. A method for evaluation of vertical crustal movements from scatted geodetic revellings. *Canadian Journal of Earth Sciences*, 11: 605-610.
34. Vaniček, P., and Krakiwsky, E., 1986. *Geodesy: The Concepts*, 2nd ed., North-Holland, Amsterdam, Netherlands.
35. Vaniček, P. and Nagy. D., 1981. On the compilation of the map of contemporary vertical crustal movements in Canada. *Tectonophysics*, 71: 75-86.
- 35A. Wojtaszczyk, P., 1997. *A mathematical Introduction to Wavelet*, Cambridge University Press, 1997
36. Zhou, J., Patrikalakis, N. M., Tuohy, S. T. and X. Ye, 1997. Scattered Data Fitting with Simplex Splines in Two and Three Dimensional Spaces. *The Visual Computer*, 13(7): 295-315.

APPENDIX

Splines

Let a be a positive real number and let $n = 0, 1, 2, \dots$ be an integer. A spline of order n with nodes in aZ is a function f defined in \mathbf{R} which is of class C^{n-1} and is a polynomial of degree at most n when restricted to each interval $[ja, (j+1)a]$ for $j \in Z$. The space of all splines of order n with nodes in aZ will be denoted by $S^n(aZ)$ [35A]. In computer graphics, a spline is a curve that connects two or more specific points, or that is defined by two or more points. The term can also refer to the mathematical equation that defines such a curve.

Consider the set of points in the illustration below.

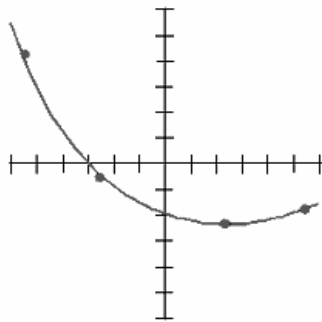


Fig. 7. Spline curve [35A]

It is easy to envision a curve (Figure 7) that approximately connects the four points. In the old days of mechanical drafting, a flexible metal or wooden strip (called a *spline*, and the term from which the present term derives) was used to construct approximate graphs such as this [35A].

Kernel

A kernel is a non-negative real valued integrable function K satisfying the following two requirements:

$$\int_{-\infty}^{+\infty} K(u) du = 1; \quad (\text{A.1})$$

$$K(-u) = K(u) \quad (\text{A.2})$$

for all values of u . The first requirement ensures that the method of kernel density estimation results in a probability density function. The second requirements ensures that the average of the corresponding distribution is equal to that of the sample used. If K is a kernel, then so is the function $K^*(u)$ defined by $K^*(u) = \lambda^{-1}K(\lambda^{-1}u)$, where $\lambda > 0$. This can be used to select a scale that is appropriate for the data [17A].